JOURNAL OF ELECTROMAGNETIC ENGINEERING AND SCIENCE, VOL. 17, NO. 2, 91~97, APR. 2017

http://dx.doi.org/10.5515/JKIEES.2017.17.2.91
ISSN 2234-8395 (Online) · ISSN 2234-8409 (Print)

Derivation of Analytic Formulas and Numerical Verification of Weakly Singular Integrals for Near-Field Correction in Surface Integral Equations

Jae-Won Rim · Il-Suek Koh*

Abstract

An accurate and efficient evaluation for hypersingular integrals (HIs), strongly singular integrals (SSIs), and weakly singular integrals (WSIs) plays an essential role in the numerical solutions of 3D electromagnetic scattering problems. We derive analytic formulas for WSIs based on Stokes' theorem, which can be expressed in elementary functions. Several numerical examples are presented to validate these analytic formulas. Then, to show the feasibility of the proposed formulations for numerical methods, these formulations are used with the existing analytical expressions of HIs and SSIs to correct the near-field interaction in an iterative physical optics (IPO) scheme. Using IPO, the scattering caused by a dihedral reflector is analyzed and compared with the results of the method of moments and measurement data.

Key Words: Iterative Physical Optics, Near-Field Correction, Singularity Subtraction, Weakly Singular Integrals.

I. INTRODUCTION

Surface integral equations (SIEs) have been used to solve 3D electromagnetic (EM) scattering problems in a variety of applications due to the efficiency of this method [1]. To solve EM scattering caused by impenetrable objects, such as perfectly electric conductors (PECs), several SIEs can be used, including the electric field integral equation (EFIE), the magnetic field integral equation (MFIE), and the combined field integral equation (CFIE). Also, the Poggio-Miller-Chang-Harrington-Wu-Tsai (PMCHWT) equation [2] or the Muller equation [3] can be employed for penetrable objects, such as dielectric bodies.

All of these equations include three types of singular integral, which consist of a double or single gradient operator on the scalar Green's function: $1/R^2$ hypersingular integrals (HSIs), $1/R^2$ strongly singular integrals (SSIs), and $1/R$ weakly singular integrals (WSIs), where R is the distance between a source point and an observation point. When the observation point is very close to the source point, near-field correction (NC) methods, such as singularity subtraction, are essential because the numerical quadrature rule may not be sufficiently accurate [4]. For example, if a method of moments (MOM) with a divergence-conforming basis function, such as Rao-Wilton-Glisson (RWG), is exploited [5], special treatment is required for the WSIs. Evaluation is also required for SSIs and HSIs in the Nystrom method [6] or in the boundary element method. Thus, the accurate and efficient treatment of HSIs, SSIs, and WSIs is important because of its significant impact on the final numerical

Manuscript received January 5, 2017 ; Revised March 23, 2017 ; Accepted April 4, 2017. (ID No. 20170105-003J)
Department of Electronic Engineering, Inha University, Incheon, Korea.
*Corresponding Author: Il-Suek Koh (e-mail: ikoh@inha.ac.kr)

This is an Open-Access article distributed under the terms of the Creative Commons Attribution Non-Commercial License (http://creativecommons.org/licenses/by-nc/3.0) which permits unrestricted non-commercial use, distribution, and reproduction in any medium, provided the original work is properly cited.
ⓒ Copyright The Korean Institute of Electromagnetic Engineering and Science. All Rights Reserved.

accuracy.

A few techniques have been developed to deal with HSIs and SSIs [7, 8]. Tong and Chew [7] have proposed a systematic solution for both types of integral. In [8], they improved on their solutions for HSIs and SSIs, which are expressed as closed-form formulations. Several analytical and numerical techniques have also been reported for WSIs in [9–14]. These techniques may, however, be inconvenient when considering implementation as they require the introduction of a polar coordinate system or extra coordinate transformation [8].

In Sections II and III, we develop analytic formulas for WSIs based on Stokes' theorem. The proposed analytic formulas for WSIs are numerically verified in Section IV. In Section V, scattering by dihedral corner reflector is analyzed by an iterative physical optics (IPO) method [15] with the proposed NC scheme, which shows the usefulness of the proposed formulations in practice.

Ⅱ. Local Coordinates

The type of SIE depends on the material properties of the scatterers. If a PEC object is considered, for example, the SIE can be an EFIE or an MFIE [1], expressed as follows:

$$\hat{n}\times jk_0 Z_0 \iint_{\Delta S}\left(\bar{I}+\frac{\vec{\nabla}\vec{\nabla}}{k^2}\right) g(\vec{r},\vec{r}')\cdot\vec{J}(\vec{r}')dS' = \hat{n}\times\vec{E}^i(\vec{r}) \tag{1}$$

$$\frac{1}{2}\vec{J}(\vec{r})+\hat{n}\times\iint_S \vec{\nabla}g(\vec{r},\vec{r}')\times\vec{J}(\vec{r}')dS' = \hat{n}\times\vec{H}^i(\vec{r}), \tag{2}$$

where k_0, Z_0, $\hat{n}$, and $\vec{J}$ are the propagation constant, intrinsic impedance, unit normal vector, and induced surface current, respectively. $\vec{E}^i$ and $\vec{H}^i$ are the incident electric and magnetic fields, respectively. $g(\vec{r},\vec{r}') = e^{jk_0R}/(4\pi R)$ is the scalar Green's function. Here, $R = |\vec{r}-\vec{r}'|$ is the distance between an observation point, $\vec{r}$, and a source point, $\vec{r}'$.

Usually, as the first step in solving the required SIEs, the object is discretized into triangular patches. Then, the interactions among the patches are calculated. When the source patch is very close to the observation patches, the computation of the interaction becomes difficult due to the singularity of the dyadic Green's function. There can be a double or single gradient operator on the scalar Green's function in Eqs. (1) and (2). Similarly, a PMCHWT equation or a Müller equation for penetrable objects has the same order of singularity as that in Eqs. (1) and (2). The singularity subtraction method [8] can be used to handle the singularity of the dyadic Green's function. For simplicity, the source patch and the observation point are transformed into local coordinates, (u, v, w) (see Fig. 1 in [8]). In these local coordinates, the required analytical formulations of the WSIs are formulated.

The double gradient on the scalar Green's function $\vec{\nabla}\vec{\nabla}g(\vec{r},\vec{r}')$ in Eq. (1) creates singularity kernels (see Eq. (9) in [8]). Once the singularity subtraction scheme is applied, HSIs, SSIs, and WSIs arise. After applying the singularity subtraction method, regular terms can be calculated by the numerical quadrature rule. However, the HSIs, SSIs, and WSIs should be evaluated analytically since they are singular. The singularity kernels generated by a single gradient on the Green's function $\vec{\nabla}g(\vec{r},\vec{r}')$ can be treated in a similar manner.

Ⅲ. Analytic Formulas for WSIs

To derive analytic WSI formulas for an arbitrarily rotated source patch in global coordinates, the vertices of the source patch and the observation point should be converted into local coordinates. Using Stokes' theorem, a surface integral over the source patch can be converted into a line integral along its boundary as

$$\iint_{\Delta S'}\left(\vec{\nabla}\times\vec{A}\right)\cdot\hat{n}dS' = \oint_{C'}\vec{A}\cdot d\vec{l}', \tag{3}$$

where $\vec{A} = A_u\hat{u}+A_v\hat{v}+A_w\hat{w}$ is a vector field in the local coordinates and $d\vec{l}$ is the path along the boundary of the patch. The source patch is assumed to be located in the uv plane so that the unit normal vector is always given as $\hat{n}=\hat{w}$. Hence, Eq. (3) can be simplified as

$$\iint_{\Delta S'}\frac{\partial A_u}{\partial v}dS' = -\oint_{C'}A_u du',\ \iint_{\Delta S'}\frac{\partial A_u}{\partial u}dS' = \oint_{C'}A_v dv'. \tag{4}$$

All HSIs, SSIs and WSIs are essential for NC. In [8], analytical formulations are derived for HSIs and SSIs. Hence, in this paper, we derive analytic formulas for WSIs. The required WSIs are summarized as follows:

$$\begin{aligned}
&I_1 = \iint_{\Delta S'}\frac{1}{R}dS',\ I_2 = \iint_{\Delta S'}\frac{(u-u')^2}{R^3}dS',\\
&I_3 = \iint_{\Delta S'}\frac{(v-v')^2}{R^3}dS',\ I_4 = \iint_{\Delta S}\frac{(u-u')(v-v')}{R^3}dS',\\
&I_5 = \iint_{\Delta S'}\frac{(u-u')}{R}dS',\ I_6 = \iint_{\Delta S'}\frac{(v-v')}{R}dS',\\
&I_7 = \iint_{\Delta S'}\frac{(u-u')(v-v')}{R}dS'.
\end{aligned} \tag{5}$$

By using Eq. (4) with the help of integral tables [16], all WSIs in Eq. (5) can be analytically evaluated. For example, I_1 can be converted using Eq. (4) into

$$I_1 = \iint_{\Delta S'}\frac{1}{R}dS' = \oint_{C'}\ln\left|R-(u-u')\right|dv'. \tag{6}$$

To calculate the closed line integral, the integral from the i^{th} vertex to the $i+1^{\text{th}}$ vertex can be written as

$$\int_{v_i}^{v_{i+1}} \ln \left| \sqrt{\begin{Bmatrix} \left(u-u_i'+\dfrac{u_{i+1}'-u_i'}{v_{i+1}'-v_i'}v_i-\dfrac{u_{i+1}'-u_i'}{v_{i+1}'-v_i'}v \right)^2 \\ +(v-v')^2+w^2 \end{Bmatrix}} \right. \left. \begin{matrix} \\ -\left(u-u_i'+\dfrac{u_{i+1}'-u_i'}{v_{i+1}'-v_i'}v_i-\dfrac{u_{i+1}'-u_i'}{v_{i+1}'-v_i'}v' \right) \end{matrix} \right| dv'. \tag{7}$$

Considering all vertices for $i=1, 2, 3$, with the aid of [16, Eqs. (602.2) and (730)] the formula for I_1 can be expressed as

$$I_1 = \sum_{i=1}^{3} \begin{bmatrix} \dfrac{A_i v - B_i}{\sqrt{1+A_i^2}} \begin{pmatrix} \ln\left| -A_iB_i + v_{i+1}' + A_i^2 v_{i+1}' - v + R_{i+1}\sqrt{1+A_i^2} \right| \\ -\ln\left| -A_iB_i + v_i' + A_i^2 v_i' - v + R_i\sqrt{1+A_i^2} \right| \end{pmatrix} \\ -w\tan^{-1}\left(\dfrac{a_i c_i}{a_i^2 + l_i^2\left(w^2 + wR_{i+1}\right)} \right) \\ -w\tan^{-1}\left(\dfrac{a_i b_i}{a_i^2 + l_i^2\left(w^2 + wR_i\right)} \right) \end{bmatrix}, \tag{8}$$

where $i+1 = \mathrm{mod}(i,3)+1$ and $\mathrm{mod}(\cdot,\cdot)$ are the modular operators since the fourth vertex is same as the first vertex. In a similar approach to that of Eqs. (6)–(8), I_2–I_7 can be derived as follows:

$$I_2 = \iint_{\Delta S'} \frac{(u-u')^2}{R^3} dS' = \oint_C \left[\frac{(u-u')}{R} + \ln\left| R-(u-u') \right| \right] dv'$$

$$= \sum_{i=1}^{3} \begin{bmatrix} -\dfrac{A_i}{\sqrt{1+A_i^2}}\left(R_{i+1}-R_i\right) + \dfrac{B_i - A_i v}{\left(1+A_i^2\right)^{3/2}} \times \\ \begin{pmatrix} \ln\left| -A_iB_i + v_{i+1}' + A_i^2 v_{i+1}' - v + R_{i+1}\sqrt{1+A_i^2} \right| \\ -\ln\left| -A_iB_i + v_i' + A_i^2 v_i' - v + R_i\sqrt{1+A_i^2} \right| \end{pmatrix} \\ +\dfrac{A_i v - B_i}{\sqrt{1+A_i^2}} \begin{pmatrix} \ln\left| -A_iB_i + v_{i+1}' + A_i^2 v_{i+1}' - v + R_{i+1}\sqrt{1+A_i^2} \right| \\ -\ln\left| -A_iB_i + v_i' + A_i^2 v_i' - v + R_i\sqrt{1+A_i^2} \right| \end{pmatrix} \\ -w\tan^{-1}\left(\dfrac{a_i c_i}{a_i^2 + l_i^2\left(w^2 + wR_{i+1}\right)} \right) \\ -w\tan^{-1}\left(\dfrac{a_i b_i}{a_i^2 + l_i^2\left(w^2 + wR_i\right)} \right) \end{bmatrix}$$

$$I_3 = \iint_{\Delta S'} \frac{(v-v')^2}{R^3} dS' = -\oint_C \left[\frac{(v-v')}{R} + \ln\left| R-(v-v') \right| \right] du'$$

$$= \sum_{i=1}^{3} \begin{bmatrix} \dfrac{C_i}{\sqrt{1+C_i^2}}\left(R_{i+1}-R_i\right) + \dfrac{C_i u - D_i}{\left(1+C_i^2\right)^{3/2}} \times \\ \begin{pmatrix} \ln\left| -C_iD_i + u_{i+1}' + C_i^2 u_{i+1}' - u + R_{i+1}\sqrt{1+C_i^2} \right| \\ -\ln\left| -C_iD_i + u_i' + C_i^2 u_i' - u + R_i\sqrt{1+C_i^2} \right| \end{pmatrix} + \\ \dfrac{C_i v - D_i}{\sqrt{1+C_i^2}} \begin{pmatrix} \ln\left| -C_iD_i + v_{i+1}' + C_i^2 v_{i+1}' - v + R_{i+1}\sqrt{1+C_i^2} \right| \\ -\ln\left| -C_iD_i + v_i' + C_i^2 v_i' - v + R_i\sqrt{1+C_i^2} \right| \end{pmatrix} \\ -w\tan^{-1}\left(\dfrac{a_i c_i}{a_i^2 + l_i^2\left(w^2 + wR_{i+1}\right)} \right) \\ -w\tan^{-1}\left(\dfrac{a_i b_i}{a_i^2 + l_i^2\left(w^2 + wR_i\right)} \right) \end{bmatrix}$$

$$I_4 = \iint_{\Delta S'} \frac{(u-u')(v-v')}{R^3} dS' = \oint_C \frac{(v-v')}{R} dv'$$

$$= \sum_{i=1}^{3} \begin{bmatrix} -\dfrac{1}{1+A_i^2}\left(R_{i+1}-R_i\right) + \dfrac{A_i\left(A_i v - B_i\right)}{\left(1+A_i^2\right)^{3/2}} \times \\ \begin{pmatrix} \ln\left| -A_iB_i + v_{i+1}' + A_i^2 v_{i+1}' - v + R_{i+1}\sqrt{1+A_i^2} \right| \\ -\ln\left| -A_iB_i + v_i' + A_i^2 v_i' - v + R_i\sqrt{1+A_i^2} \right| \end{pmatrix} \end{bmatrix}$$

$$I_5 = \iint_{\Delta S'} \frac{(u-u')}{R} dS' = -\oint_C R dv'$$

$$= \sum_{i=1}^{3} \begin{bmatrix} -\dfrac{1}{2\left(1+A_i^2\right)} \begin{bmatrix} \left(-A_iB_i + v_{i+1}' + A_i^2 v_{i+1}' - v \right) R_{i+1} \\ -\left(-A_iB_i + v_i' + A_i^2 v_i' - v \right) R_i \end{bmatrix} \\ -\dfrac{\left(B_i - A_i v\right)^2 + \left(1+A_i^2\right)w^2}{2\left(1+A_i^2\right)^{3/2}} \times \\ \begin{bmatrix} \ln\left| -A_iB_i + v_{i+1}' + A_i^2 v_{i+1}' - v + R_{i+1}\sqrt{1+A_i^2} \right| \\ -\ln\left| -A_iB_i + v_i' + A_i^2 v_i' - v + R_i\sqrt{1+A_i^2} \right| \end{bmatrix} \end{bmatrix}$$

$$I_6 = \iint_{\Delta S'} \frac{(v-v')}{R} dS' = \oint_C R du'$$

$$= \sum_{i=1}^{3} \begin{bmatrix} \dfrac{1}{2\left(1+C_i^2\right)} \begin{bmatrix} \left(-C_iD_i + u_{i+1}' + C_i^2 u_{i+1}' - u \right) R_{i+1} \\ -\left(-C_iD_i + u_i' + C_i^2 u_i' - u \right) R_i \end{bmatrix} \\ +\dfrac{\left(D_i - C_i u\right)^2 + \left(1+C_i^2\right)w^2}{2\left(1+C_i^2\right)^{3/2}} \times \\ \begin{bmatrix} \ln\left| -C_iD_i + u_{i+1}' + C_i^2 u_{i+1}' - u + R_{i+1}\sqrt{1+C_i^2} \right| \\ -\ln\left| -C_iD_i + u_i' + C_i^2 u_i' - u + R_i\sqrt{1+C_i^2} \right| \end{bmatrix} \end{bmatrix}$$

$$I_7 = \iint_{\Delta S'} \frac{(u-u')(v-v')}{R} dS' = -\oint_C (v-v') R dv'$$

$$= \sum_{i=1}^{3} \begin{bmatrix} \dfrac{R_{i+1}}{6\left(1+A_i^2\right)^2} \begin{pmatrix} \left(2-A_i\right)^2 B_i^2 + 2\left(1+A_i^2\right)^2 v_{i+1}'^2 \\ -\left(4+7A_i^2+3A_i^4\right) v v_{i+1}' + \\ 2v^2 + 2w^2 + 5A_i^2 v^2 - A_iB_i \\ \left(v_{i+1}' + A_i^2 v_{i+1}' + 3v - 3A_i^2 v \right) \\ +2A_i^2 w^2 \end{pmatrix} - \\ \dfrac{R_i}{6\left(1+A_i^2\right)^2} \begin{pmatrix} \left(2-A_i\right)^2 B_i^2 + 2\left(1+A_i^2\right)^2 v_i'^2 - \\ \left(4+7A_i^2+3A_i^4\right) v v_i' + 2v^2 + \\ 2w^2 + 5A_i^2 v^2 + 2A_i^2 w^2 - \\ A_iB_i\left(v_i' + A_i^2 v_i' + 3v - 3A_i^2 v \right) \end{pmatrix} \\ +\dfrac{A_i\left(B_i - A_i v\right)\left(\left(B_i - A_i v\right)^2 + \left(1+A_i^2\right)^2\right)}{2\left(1+A_i^2\right)^{5/2}} \\ \times \begin{Bmatrix} \ln\left| -A_iB_i + v_{i+1}' + A_i^2 v_{i+1}' - v + R_{i+1}\sqrt{1+A_i^2} \right| \\ -\ln\left| -A_iB_i + v_i' + A_i^2 v_i' - v + R_i\sqrt{1+A_i^2} \right| \end{Bmatrix} \end{bmatrix} \tag{9}$$

where

$$A_i = \frac{u_{i+1}' - u_i'}{v_{i+1}' - v_i'},\ B_i = u - u_i' + A_i v_i'$$

$$C_i = \frac{v_{i+1}' - v_i'}{u_{i+1}' - u_i'},\ D_i = v - v_i' + C_i u_i'$$

$$R_i = \sqrt{\left(u - u_i'\right)^2 + \left(v - v_i'\right)^2 + w^2}$$

$$l_i = \sqrt{\left(u_{i+1}' - u_i'\right)^2 + \left(v_{i+1}' - v_i'\right)^2}$$

$$a_i = \left(u_i' - u\right)\left(v_{i+1}' - v_i'\right) - \left(v_i' - v_0\right)\left(u_{i+1}' - u_i'\right)$$

$$b_i = \left(u_{i+1}' - u_i\right)\left(u_i' - u\right) + \left(v_{i+1}' - v_i\right)\left(v_i' - v\right)$$

$$c_i = \left(u_{i+1}' - u_i\right)\left(u_{i+1}' - u\right) + \left(v_{i+1}' - v_i\right)\left(v_{i+1}' - v\right).$$

Ⅳ. Numerical Verification of WSIs

Gauss quadrature rule is very efficient for the numerical computation of surface integrals [14]. Its accuracy, however, is degenerated in the near-singular case, in which the distance between the observation point and the source point is minimal. The criteria of the near-singular case depend on the dimensions of the source patch. To improve the accuracy of the quadrature rule, the source patch is divided into many small sub-patches. Then, the low-order quadrature method is applied to each sub-triangle patch, which may be numerically inefficient, but accuracy can be guaranteed if the convergence of the numerical value is achieved. Over the sub-patches, the current is assumed to be a constant.

A source patch is located at the *uv* plane, whose three vertices are given as $p_1(0.7\lambda, 0.1\lambda, 0)$, $p_2(0.4\lambda, 0.3\lambda, 0)$, and $p_3(0.1\lambda, 0.2\lambda, 0)$, respectively. The observation point is at $p_0(0.4\lambda, 0.2\lambda, w_0)$, where w_0 varies from 1λ to 0.01λ.

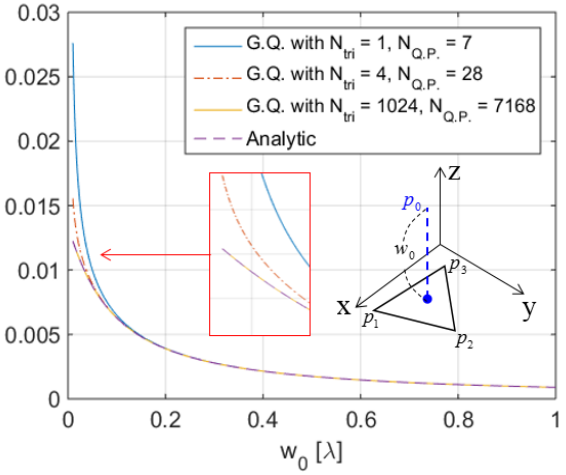

Fig. 1. Numerical comparison for I_1. The analytic solution is compared with the results of the numerical quadrature rule, with $N_{tri} = 1{,}024 / N_{Q.P.} = 7{,}168$.

In Fig. 1, the analytic and numerical results for I_1 are compared. It is evident that I_1 increases as w_0 decreases since the distance between the observation point and the source patch, R, decreased. As the number of sub-triangle patches, N_{tri}, increases, the numerical accuracy of the quadrature rule is improved because the effective number of quadrature points, $N_{Q.P.}$, increases. It can be observed that the analytic result of I_1 is in good agreement with the numerical results when $N_{tri} = 1{,}024 / N_{Q.P.} = 7{,}168$, even for the near-singular case.

For the verification of I_1–I_7 in Eq. (9), therefore, the Gauss quadrature method is adopted with the assumption that $N_{tri} = 1{,}024 / N_{Q.P.} = 7{,}168$. The simulation parameters are the same as those in Fig. 2. Fig. 3 shows the relative error, ε, as a function of w_0, where the maximum error is less than 10^{-4}. To consider the effect of the observation point location, the source patch is randomly rotated, and then the same computation as that in Fig. 2 is performed. Fig. 3 presents a relative error comparison in which the maximum error is still less than 10^{-4}. Therefore, Eq.

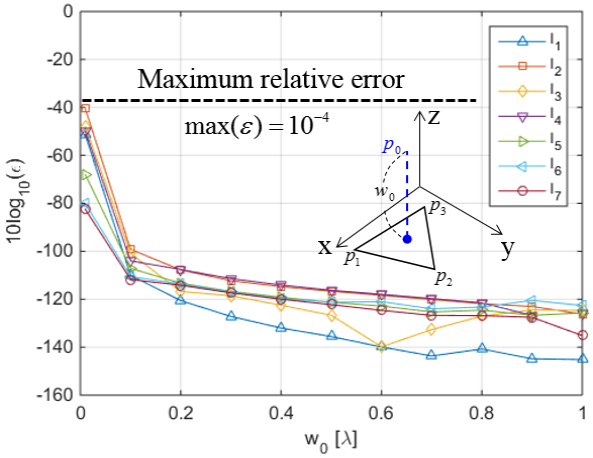

Fig. 2. Relative error of WSIs, I_1–I_7, comparing analytic and numerical results.

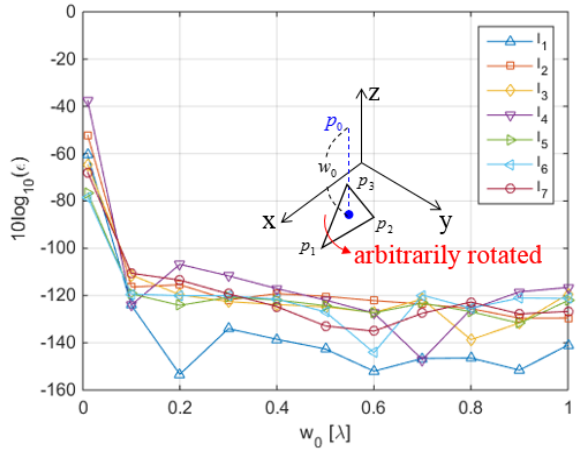

Fig. 3. Relative error of WSIs, I_1–I_7, for an arbitrarily rotated triangle source patch.

(9) can be exact for any source patch as well as for the configuration of the observation point.

V. The Application of NC to IPO

For HSI and SSI formulations, the proposed analytical expression of WSIs can be completed for the NC in scattering applications. To show the feasibility of applying the proposed formulations to realistic EM problems, the NC is considered for the IPO method [15]. The IPO formulation is based on Eq. (2) to iteratively calculate the current in a PEC body. The updated equation is expressed as follows:

$$\vec{J}_n(\vec{r}) = \vec{J}_{n-1}(\vec{r}) - \frac{1}{2\pi}\iint_{S'} \begin{bmatrix} \hat{n}(\vec{r}) \times \left(\vec{R} \times \vec{J}_{n-1}(\vec{r}')\right) \\ \cdot (1 - jk_0 R)\dfrac{e^{jk_0 R}}{R^3} \end{bmatrix} dS', \tag{10}$$

where $\vec{J}_0(\vec{r}) = 2\hat{n}(\vec{r}) \times \vec{H}^i(\vec{r})$ and $\hat{n}(\vec{r})$ are the first-order PO current and unit normal vector, respectively. Since Eq. (10) includes singularities, the formulations in Section III can be used to correct these singularities.

For the numerical simulation, we consider a dihedral corner reflector whose corner angle is 60°. The operating frequency is 5 GHz, and the length of one side of the reflector is 20 cm ($\approx 3.5\lambda$). The reflector is oriented toward $\theta = 90^\circ$ and has a direction of $\phi = 90^\circ$; the wave is incident from $\theta = 90^\circ$ and has a direction of $\phi = 90^\circ$. The bistatic radar cross section (RCS) is calculated along the principal cut ($\phi = 0^\circ$ to $\phi = 180^\circ$) at $\theta = 90^\circ$ for both V and H polarizations.

The IPO results are compared with both the MOM and measurement results. Here, the MOM solution is based on the EFIE. For the measurements, a standard horn antenna is used with a half power beamwidth of 20°. Short-open-load-thru (SOLT) calibration is used for vector network analyzer (VNA) calibration, and a 30-cm-by-20-cm rectangular plate is used to calibrate the target RCS level. The measurement distance between the antenna and the target is 3 m, and signals from 5.5 m to 6.5 m are range-gated. The RCS is measured from $\phi = 30^\circ$ to $\phi = 150^\circ$ at $\theta = 90^\circ$ with a 2° sampling rate. Fig. 4 shows the comparison of the results of the IPO method with and without the NC scheme, the MOM and the measurement results.

The IPO method in combination with the NC scheme can provide much more accurate results than the same method without the NC scheme, as shown in Fig. 4. Since the corner angle is 60°, the interaction around the corner may be very

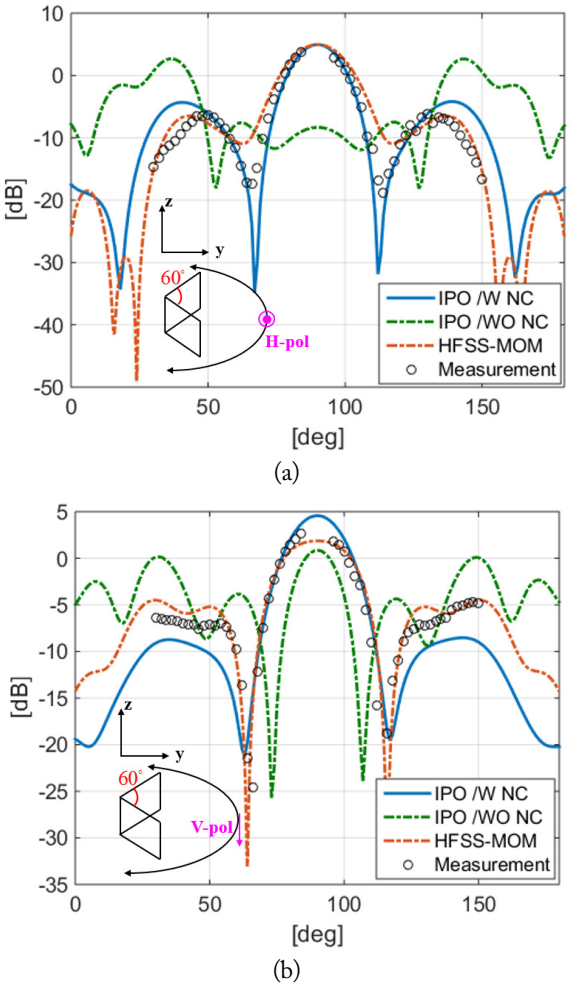

Fig. 4. Comparison of the bistatic radar cross section (RCS) of a dihedral corner reflector by iterative physical optics (IPO) with and without near-field correction (NC), method of moments (MOM), and measurements: (a) HH and (b) VV.

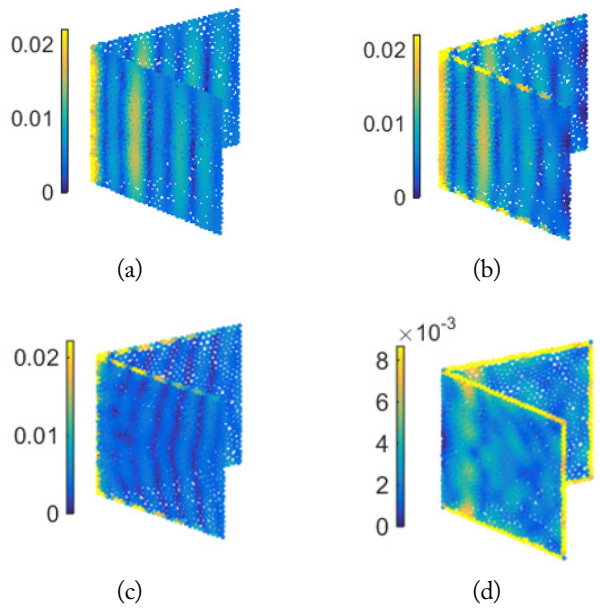

Fig. 5. Comparison of the surface current distributions of an (a) IPO with NC (HH) and (b) MOM (HH) dihedral corner reflector; (c) current difference between IPO with NC and MOM for HH polarization; (d) current difference between IPO with NC and MOM for VV polarization.

strong. In Fig. 5, which shows the induced surface current distribution of the corner reflector, the IPO method with the NC scheme can estimate the current accurately, especially around the corner, as expected. The HH and VV results given by the IPO method with NC have discrepancies since the IPO formulation is based on the MFIE whereas the MOM is based on the EFIE. This is because the MOM based on an EFIE provides a stable solution, but the MOM based on an MFIE is unstable: The thickness of the dihedral corner reflector is very thin (almost zero). Since the MFIE generally provides an accurate solution only when the scatterer surface is sufficiently smooth and closed, the current distributions analyzed by the IPO method with NC are quite inaccurate at the edges when compared to the MOM currents (Fig. 5(c) and (d)) The current difference causes discrepancies.

It can be observed that the VV results from IPO with the NC scheme contain more errors than the HH results. One explanation is that, for the VV case, the difference of current distribution between the MOM and IPO with NC is greater around the edges because the incident wave is polarized in the direction in which the polarization perfectly coincides with the edge; this may induce strong fringe currents [17] on the edge (Fig. 5(d)) and cause quite a strong diffraction effect.

VI. Conclusion

We have derived analytic formulas for WSIs based on Stokes' theorem for NC. To validate the proposed formulas for WSIs, serval numerical examples are presented, showing that the maximum error is less than 10^{-4} for any configuration of the source patch or the observation point. For an EM scattering application, dihedral scattering is considered. The results of the IPO method with and without the NC scheme are compared with MOM results and measurement data. It can be observed that the NC is crucial if strong interactions exist. Hence, the proposed formulation can be used in conjunction with any numerical method for SIEs to improve the accuracy of these methods.

This work was supported by ICT R&D program of MSIP/IITP. (B0717-16-0045, Cloud based SW platform development for RF design and EM analysis).

References

[1] W. C. Gibson, *The Method of Moments in Electromagnetics*. Boca Raton, FL: Chapman and Hall/CRC, 2007.

[2] A. J. Poggio and E. K. Miller, "Integral equation solutions of three-dimensional scattering problems," in *Computer Techniques for Electromagnetics*, R. Mittra, Ed. Oxford: Pergamon Press, 1973, pp. 159-260.

[3] C. Muller, *Foundations of the Mathematical Theory of Electromagnetic Waves*. Berlin: Springer-Verlag, 1969.

[4] D. Dunavant, "High degree efficient symmetrical Gaussian quadrature rules for the triangle," *International Journal for Numerical Methods in Engineering*, vol. 21, no. 6, pp. 1129–1148, 1985.

[5] S. M. Rao, D. R. Wilton, and A. W. Glisson, "Electromagnetic scattering by surfaces of arbitrary shape," *IEEE Transactions on Antenna and Propagation*, vol. 30, no. 3, pp. 409–418, 1982.

[6] L. F. Canino, J. J. Ottusch, M. A. Stalzer, J. L. Visher, and S. M. Wandzura, "Numerical solution of the Helmholtz equation in 2D and 3D using a high-order Nyström discretization," *Journal of Computational Physics*, vol. 146, no. 2, pp. 627–663, 1998.

[7] M. S. Tong and W. C. Chew, "Super-hyper singularity treatment for solving 3D electric field integral equations," *Microwave and Optical Technology Letters*, vol. 49, no. 6, pp. 1383–1388, 2007.

[8] M. S. Tong and W. C. Chew, "A novel approach for evaluating hypersingular and strongly singular surface integrals in electromagnetics," *IEEE Transactions on Antennas and Propagation*, vol. 58, no. 11, pp. 3593–3601, 2010.

[9] D. R. Wilton, S. M. Rao, A. W. Glisson, D. H. Schaubert, O. M. Al-Bundak, and C. M. Butler, "Potential integrals for uniform and linear source distributions on polygonal and polyhedral domains," *IEEE Transactions on Antennas and Propagation*, vol. 32, no. 3, pp. 276–281, 1984.

[10] C. Schwab and W. L. Wendland, "On numerical cubatures of singular surface integrals in boundary element methods," *Numerische Mathematik*, vol. 62, no. 1, pp. 343–369, 1992.

[11] R. D. Graglia, "On the numerical integration of the linear shape functions times the 3-D Green's function or its gradient on a plane triangle," *IEEE Transactions on Antennas and Propagation*, vol. 41, no. 10, pp. 1448–1455, 1993.

[12] A. Herschlein, J. V. Hagen, and W. Wiesbeck, "Methods for the evaluation of regular, weakly singular and strongly singular surface reaction integrals arising in method of moments," *Applied Computational Electromagnetics Society Journal*, vol. 17, no. 1, pp. 63–73, 2002.

[13] B. M. Johnston and P. R. Johnston, "A comparison of transformation methods for evaluation two-dimensional weakly singular integrals," *International Journal for Numerical Methods in Engineering*, vol. 56, no. 4, pp. 589–607, 2003.

[14] M. G. Duffy, "Quadrature over a pyramid or cube of integrands with a singularity at a vertex," *SIAM Journal on Numerical Analysis*, vol. 19, no. 6, pp. 1260–1262, 1982.

[15] F. Obelleiro-Basteiro, J. L. Rodriguez, and R. J. Burkholder, "An iterative physical optics approach for analyzing the electromagnetic scattering by large open-ended cavities," *IEEE Transactions on Antennas and Propagataion.*, vol. 43, no.4, pp. 356–361, 1995.

[16] H. B. Dwight, *Tables of Integrals and Other Mathematical Data*, 4th ed. New York, NY: Macmillan, 1961.

[17] P. Y. Ufimtsev, *Fundamentals of the Physical Theory of Diffraction.* Hoboken, NJ: John Wiley & Sons, 2007.

Jae-Won Rim

received B.S. and M.S. degrees in electronic engineering from Inha University, Incheon, Korea in 2014 and 2016, respectively. He is currently working toward a Ph.D. in the department of electronic engineering, Inha University, Incheon, Korea. His research interests include modeling simulations for electronic warfare and numerical techniques in electromagnetics.

Il-Suek Koh

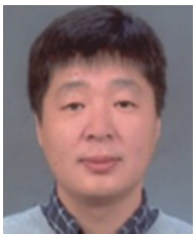

received B.S. and M.S. degrees in electronic engineering from Yonsei University, Seoul, Korea in 1992 and 1994, respectively, and he obtained his Ph.D. degree from the University of Michigan, Ann Arbor, MI, USA in 2002. In 1994, he joined LG Electronics Ltd., Seoul, as a Research Engineer. Currently, he is a professor at Inha University, Incheon, Korea. His research interests include wireless communication channel modeling and numerical and analytical methods for electromagnetic fields.